European Review for Medical and Pharmacological Sciences 2021; 25: 301-312

Uncovering the differentially expressed genes and pathways involved in the progression of stable coronary artery disease to acute myocardial infarction using bioinformatics analysis

S.-J. XIAO[1], Y.-F. ZHOU[2], Q. WU[1], W.-R. MA[1], M.-L. CHEN[2], D.-F. PAN[1]

[1]Department of Cardiology, The Affiliated Hospital of Xuzhou Medical University, Xuzhou, Jiangsu, China
[2]Department of Cardiology, The First Affiliated Hospital of Nanjing Medical University, Nanjing, Jiangsu, China

Abstract. – OBJECTIVE: Coronary artery disease (CAD) is the main cause of mortality worldwide. How stable coronary artery disease (SCAD) progresses to acute myocardial infarction (AMI) is not known. This study was aimed to explore the differentially expressed genes (DEGs) and pathways involved in the progression of SCAD to AMI.

MATERIALS AND METHODS: Publicly available gene-expression profiles (GSE71226, GSE97320, GSE66360) were downloaded from the Gene Expression Omnibus (GEO) database and integrated to identify DEGs. The GSE59867 dataset was further used to verify the result of screened DEGs. Functional-enrichment analyses, protein-protein interaction network, microRNA-transcription factor (TF)-mRNA regulatory network, and drug-gene network were visualized.

RESULTS: Sixty common DEGs (CDEGs) were screened between the SCAD-Control group and AMI-Control group in the integrated dataset. Four upregulated DEGs were selected from GSE59867. Twenty hub genes were discovered, and three significant modules were constructed in the PPI network. The intersection of functional and pathway-enrichment analyses of 60 CDEGs and the module DEGs indicated that they were mainly involved in "inflammatory response", "immune response", and "cytokine-cytokine receptor interaction". A miRNA-TF-mRNA regulatory network comprised 87 miRNAs, 16 upregulated target DEGs and 7 TFs.

CONCLUSIONS: We identified several important genes and miRNAs involved in the progression of SCAD to AMI: platelet activating factor receptor (PTAFR), aquaoporin-9 (AQP9), toll-like receptor-4 (TLR4), human constitutive androstane receptor-3 (HCAR3), leucine-rich-α2 glycoprotein-1 (LRG1), mothers Against Decapentaplegic Homolog 4 (SMAD4) and miRNA-149-5p, miRNA-6778-3p, and miRNA-520a-3p. Inflammation and the immune response had important roles in the progression from SCAD to AMI.

Key Words:
Acute myocardial infarction, Differentially expressed genes, MiRNA-transcription factor-mRNA regulatory network, Pathways, Protein-protein interaction network.

Introduction

Coronary artery disease (CAD) is one of the leading causes of death worldwide[1,2]. CAD comprises stable/unstable angina, sudden cardiac death, and myocardial infarction (MI). The pathological foundation of CAD is the formation of atherosclerotic plaques that lead to narrowing/blockage of lumina[3,4]. However, the most common cause of acute myocardial infarction (AMI) is the rupture of atherosclerotic plaques and thrombosis that blocks coronary arteries[5].

The diagnosis and management of AMI have progressed substantially in recent years. Nevertheless, the reason why atherosclerotic plaques in patients with stable coronary artery disease develop into unstable atherosclerotic plaques is not known[6]. Several biomarkers, including genes and microRNAs and their pathways, are involved in AMI progression. These include C-C motif chemokine (CCL)22, C-C chemokine receptor type (CCR)4, microRNA-124-3p,

Corresponding Author: Defeng Pan, Ph.D; e-mail: xzdefengpan@yahoo.com; xb@xzhmu.edu.cn

and the nuclear factor-kappa B (NF-κB) signaling pathway[7-9]. However, a specific diagnostic biomarker that can be used to identify patients with angina pectoris who are at risk of developing AMI is not available.

High-throughput sequencing is a very effective, accurate, and convenient way to explore gene-expression profiles by bioinformatics analysis[10]. Using the GSE71226 microarray dataset (hereafter termed "datasets"), Wang et al[11] demonstrated that expression of matrix metallopeptidase (MMP)9 and C-X-C motif chemokine receptor (CXCR)1 was upregulated significantly in stable coronary artery disease (SCAD) samples compared with that in control samples using real-time Reverse Transcription-quantitative Polymerase Chain Reaction (RT-qPCR). Using the GSE97320 dataset, Su et al[12] suggested that signal transducer and activator of transcription (STAT)3 might be the biomarker for the diagnosis and prognosis of AMI among a Chinese population. Using the GSE66360 dataset, Vijay[13] found that differentially expressed genes (DEGs), such as c-x-c motif chemokine ligand (CXCL)2, matrix metallopeptidase (MMP)9, toll-like receptor (TLR)2 and TLR4 were enriched significantly in the inflammatory response, immune response, and interactions between cytokines and cytokine receptors. However, the GSE71226, GSE97320 and GSE66360 datasets have not been further explored or compared.

We integrated the datasets described above to identify the pivotal genes and pathways related with the progression from SCAD to AMI. Also, the GSE59867 dataset was used to verify the results of screened DEGs. Common differentially expressed genes (CDEGs) and enrichment analyses were likely to be associated with the occurrence and progression from SCAD to AMI.

Materials and Methods

Data were retrieved from publicly accessible databases on the Internet. We did not require ethical approval or patient consent for use of such data.

Microarray Data

The gene-expression profiles of GSE71226, GSE97320 and GSE66360 datasets were collected from Gene Expression Omnibus (GEO)[14]. These datasets were sequenced by the GPL570-Affymetrix Human Genome U133 plus 2.0 Array [HG-U133_Plus_2]. Moreover, the GSE59867 dataset was obtained from GEO and sequenced on the platform of the GPL6244-Affymetrix Human Gene 1.0 ST Array [HuGene-1_0-st]. The GSE71226 dataset comprised peripheral-blood samples from three healthy individuals and three SCAD patients with coronary stenosis >50%. The GSE97320 dataset contained peripheral-blood samples from three normal controls and three AMI patients. The GSE66360 dataset consisted of peripheral blood from 49 patients with MI and 50 healthy controls. Additionally, the GSE59867 dataset comprised peripheral-blood samples from patients (n = 111) with ST-segment elevation myocardial infarction and patients (n = 46) with SCAD without a history of MI.

Study Design and Identification of Differentially Expressed Genes

The experimental workflow is shown as Figure 1. The original files in CEL format were transformed into an expression value matrix using the Affy package in R (R Project for Statistical Computing, Vienna, Austria) with the RMA method (to normalize expression values) and the SVA method (to remove batch differences)[15]. After merging the three datasets (GSE71226, GSE97320, GSE66360), batch effects were adjusted by the "combat" function of the "sva" package of R using empirical Bayes frameworks[16]. Analyses of DEGs were conducted using the "limma" package of R[17]. p-value < 0.05 and $|\log_2$ fold change$|$ >1 were the inclusion criteria to screen out DEGs. Volcano plots and heatmaps were visualized. The CDEGs between the SCAD-Control group and AMI-Control group were obtained for further analyses. The GSE59867 dataset was pre-processed with the "limma" package in R with the same processes and cutoff criteria as described above.

Enrichment Analyses of Common Differentially Expressed Genes

We wished to analyze the biofunction of CDEGs. Hence, the Database for Annotation, Visualization and Integrated Discovery (DAVID)[18] and KOBased Annotation System (KOBAS) online webtools[19] were applied for pathway-enrichment analyses using Gene Ontology (GO) and Kyoto Encyclopedia of Genes and Genomes (KEGG) databases[20], respectively. p-value < 0.05 and counts ≥2 were considered significant.

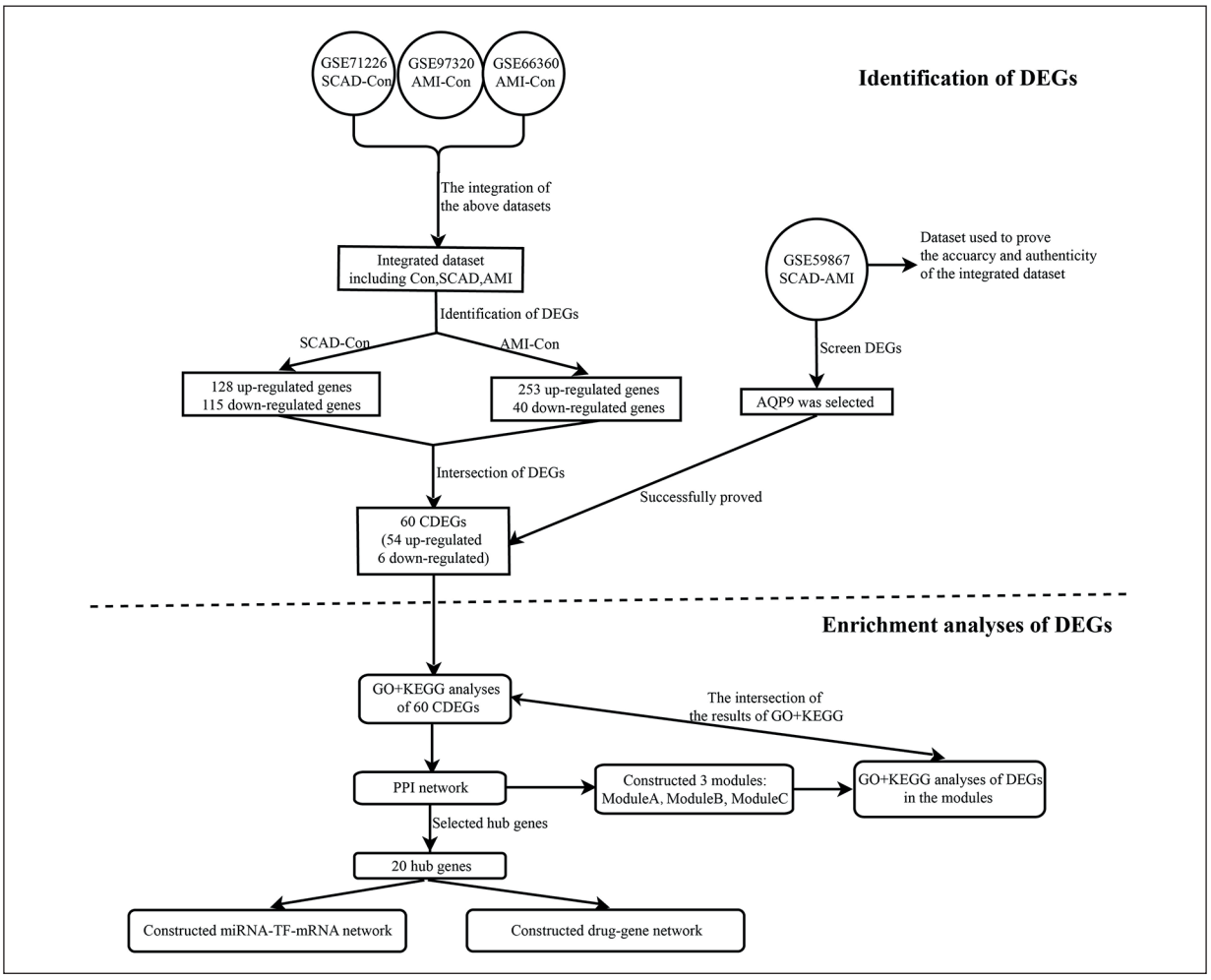

Figure 1. Study flowchart. Abbreviations: CAD: coronary artery disease; SCAD: stable coronary artery disease; AMI: acute myocardial infarction; DEGs: differentially expressed genes; CDEGs: common differentially expressed genes; GO: Gene Ontology; KEGG: Kyoto Encyclopedia of Genes and Genomes; PPI: protein-protein interaction; miRNA: MicroRNA; TF: transcription factor.

Protein-Protein Interaction (PPI) Network

Interactions between proteins were evaluated using the Search Tool for the Retrieval of Interacting Genes/Proteins (STRING) database[21]. After setting the parameter of PPI score (medium confidence) as 0.4 and removing the hidden disconnected nodes, the final PPI network was constructed and visualized by Cytoscape 3.7.1[22]. Hub genes in the network with degree ≥5 were selected. With the default parameters (degree cutoff ≥2, cutoff of node score ≥0.2, K-core ≥2, maximum depth = 100), the Cytoscape Molecular Complex Detection (MCODE) plugin was used to analyze important modules. Moreover, the genes in the module were conducted *via* pathway-enrichment analyses using the GO and KEGG databases.

Construction of a mRNA-miRNA Network

To increase the accuracy of prediction, the targeted miRNAs were predicted by the intersection of the results of miRTarbase[23], miRWalk[24], StarBase[25] and miRDB[26]. Each pair of miRNAs and mRNAs was constructed by Cytoscape subsequently.

Analyses of the miRNA-Transcription Factor (TF)-mRNA Regulatory Network

Hub genes were uploaded to the Enrichr database and the TFs targeting the hub genes were predicted[27]. p-value < 0.05 was adopted to screen the predicted TFs. MiRNA-TF-mRNA regulatory relationships were obtained using Cytoscape.

Analyses of Drug-Gene Networks

A database of drug-gene interactions (DGIdb; www.dgidb.org) was established for combined gene druggability and drug-gene interactions from several data sources[28]. The pivotal genes in the PPI network were imported into the DGIdb database, and drug-gene pairs were predicted. Cytoscape was used to construct the drug-gene network.

Statistical Analysis

p-value < 0.05 was selected to indicate a statistically significant result.

Results

Identification of DEGs

A total of 128 upregulated and 115 downregulated DEGs were selected from the control group and SCAD patients with coronary stenosis >50% in the integrated dataset (Figure 2A). In addition, 293 DEGs were screened out from normal controls and AMI patients (expression of 253 genes was upregulated and expression of 40 genes was downregulated) (Figure 2B). However, only four genes whose expression was upreg-

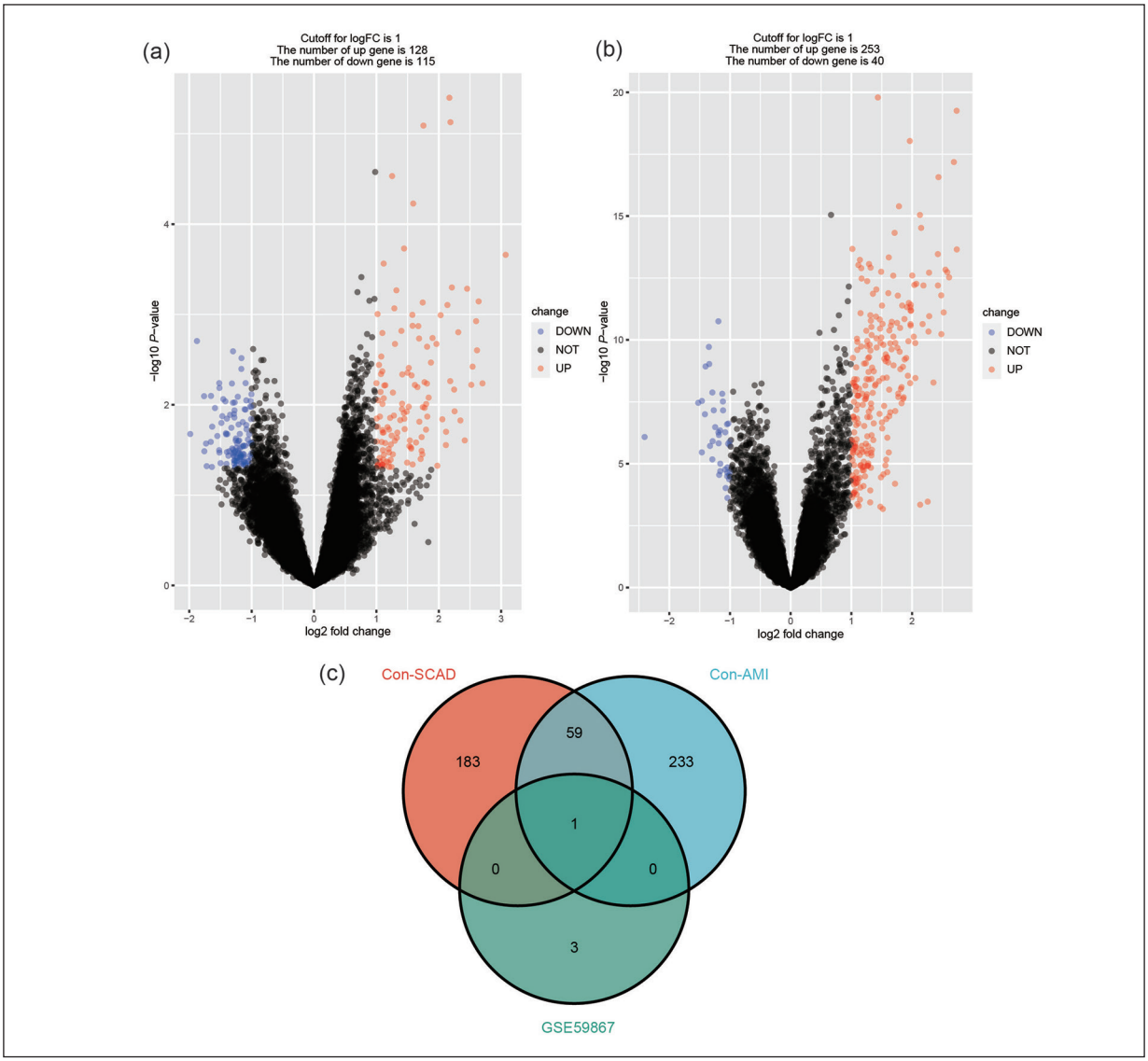

Figure 2. Volcano plots (a: SCAD vs. control; b: AMI vs. control) and Venn diagram (c) of differentially expressed genes. **A,** Volcano plots of the DEGs screened from the SCAD–Control group. **B,** Volcano plots of the DEGs screened from the AMI-Control group. Red dots and blue dots present genes with upregulated and downregulated expression, respectively. **C,** Venn diagram of the common upregulated and downregulated DEGs from the integrated dataset and GSE59867 dataset. Abbreviations: See Figure 1.

ulated genes were screened from the GSE59867 dataset: aquaporin (AQP)9, eosinophil cationic-related protein (ECRP), HP (Haptoglobin) and suppressor of cytokine signaling (SOCS3). The overlapping upregulated and downregulated DEGs obtained from the integrated dataset and GSE59867 dataset are presented in Figure 2C and **Supplementary Table I**. A heatmap representing the CDEGs between the SCAD-Control group and AMI-Control group is shown as Figure 3.

Functional-Enrichment Analyses

The enriched GO terms were classified into Biological Process (BP), Cell Component (CC) and Molecular Function (MF). The CDEGs were en-

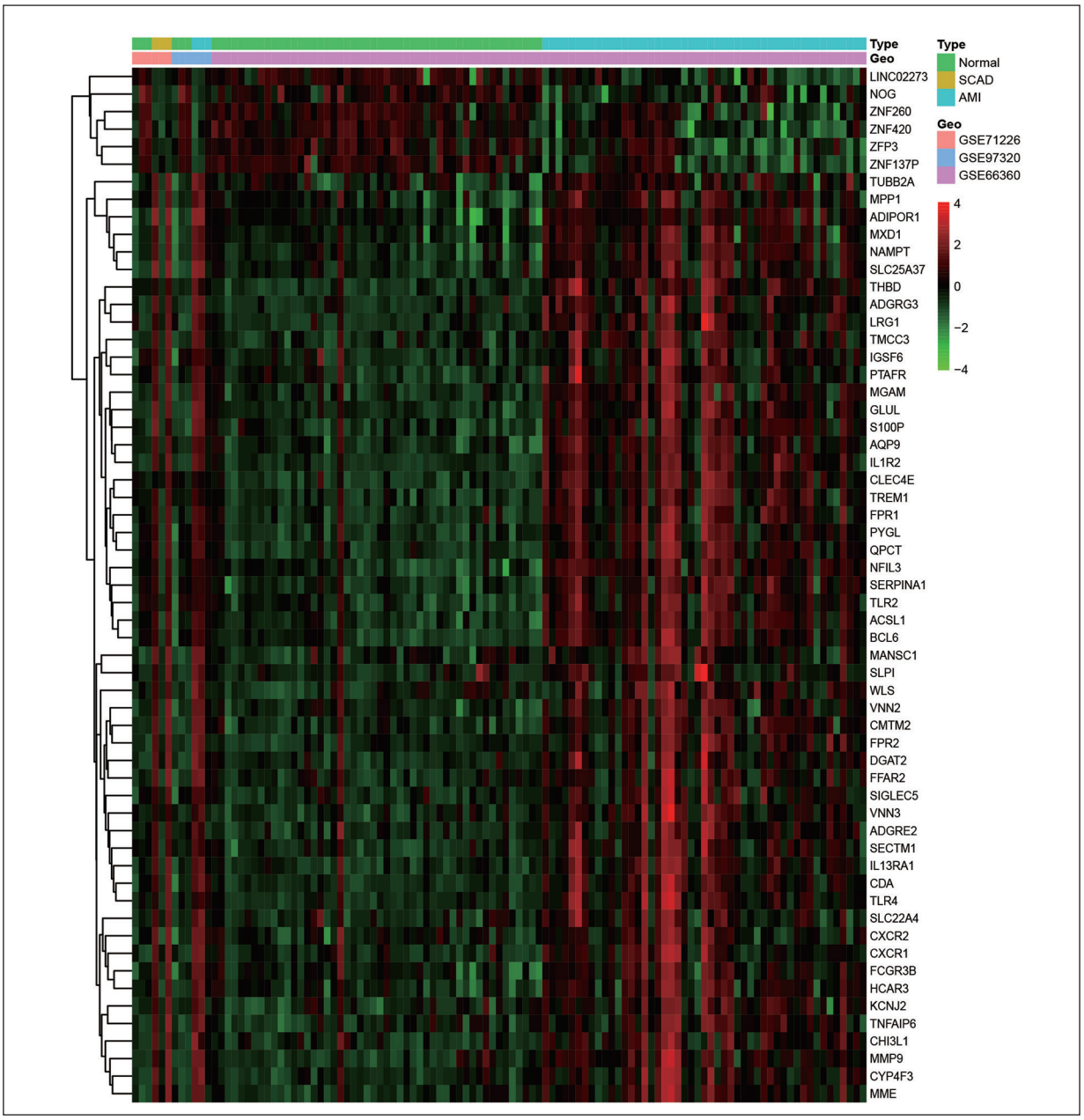

Figure 3. Heat map of common differentially expressed genes. Cluster heatmaps of the common DEGs from three datasets (GSE71266, GSE97320, GSE66360). Each row represents DEGs, and each column represents one of the samples of normal individuals or patients. Red regions denote that the expression of genes was relatively upregulated and green regions indicate that the expression of genes was relatively downregulated. Abbreviations: GEO: Gene Expression Omnibus; Others: See Figure 1.

riched mainly in BP terms such as "inflammatory response" and "immune response". For the CC ontology, the CDEGs were enriched significantly in "plasma membrane". MF analyses showed that the DEGs were mostly enriched in "lipopolysaccharide receptor activity" (Figure 4 and **Supplementary Table II**). Pathway-enrichment analyses using the KEGG database indicated that the CDEGs were involved in "metabolic pathways", "phagosome", and "cytokine-cytokine receptor interaction" (Figure 4 and **Supplementary Table III**).

Construction of a PPI Network, Hub-Gene Selection and Module Analyses

The PPI network was constructed with 39 nodes (39 upregulated) and 115 edges. By use of the MCODE plugin, three significant modules were screened from the PPI network. The most significant module had 11 nodes and 43 edges. The second most significant module contained six nodes and 11 edges. The third most significant module comprised three nodes and three edges (Figure 5A). The genes in the three significant modules were enriched mainly in "inflammatory response", "immune response" and "cytokine-cytokine receptor interaction" (**Supplementary Tables IV** and **V**). Genes with degree ≥5 were considered to be hub genes in the PPI network (Figure 5B).

Analyses of the miRNA-TF-mRNA Regulatory Network

A regulated miRNA-TF-mRNA network was built by Cytoscape that consisted of 110 nodes

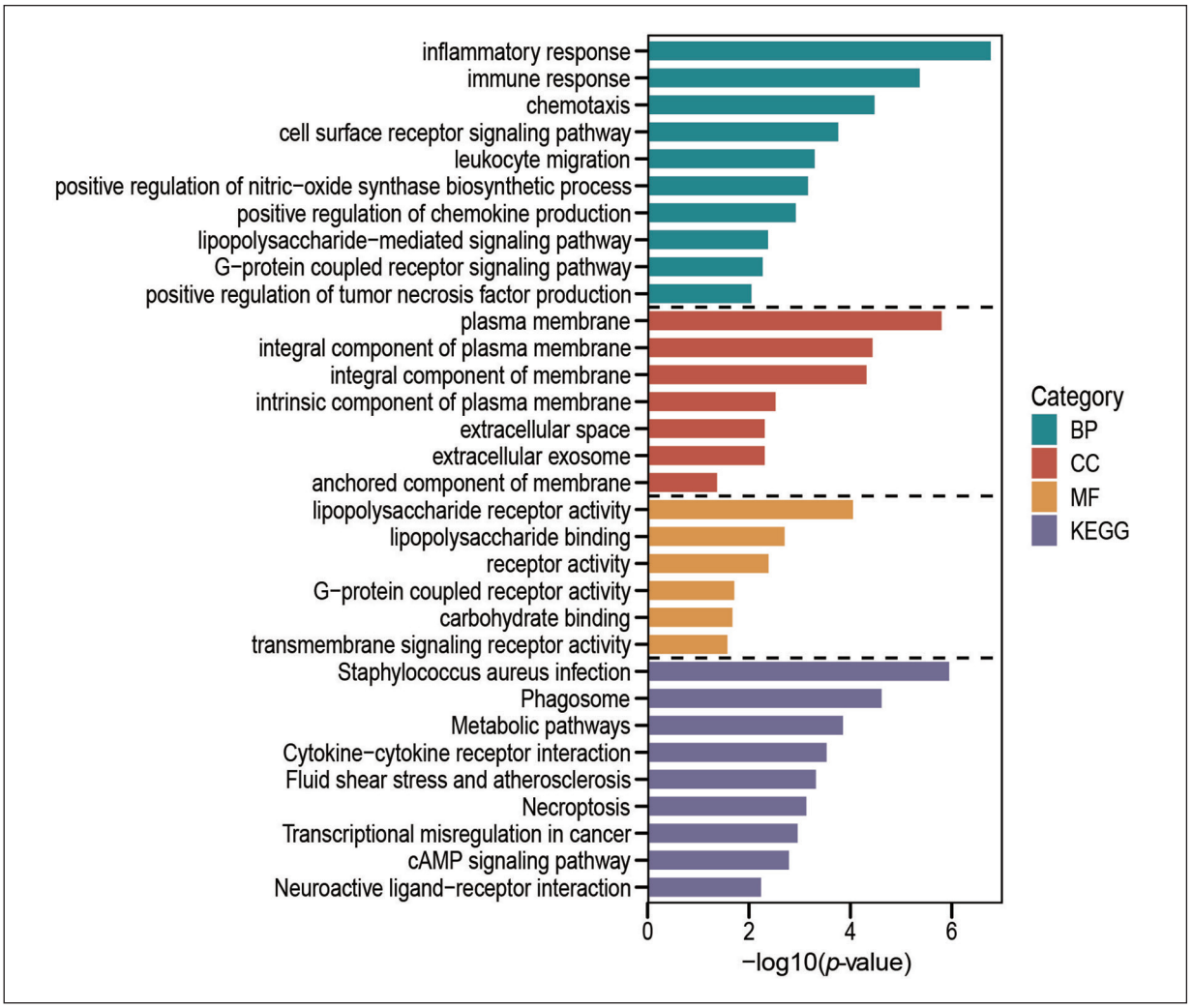

Figure 4. Common differentially expressed genes according to the GO and KEGG databases. Different colors represent the main categories of GO terms: BP, CC and MF as well as KEGG pathways. Abbreviations: BP, biological process; CC, cellular component; MF, molecular function; Others: See Figure 1.

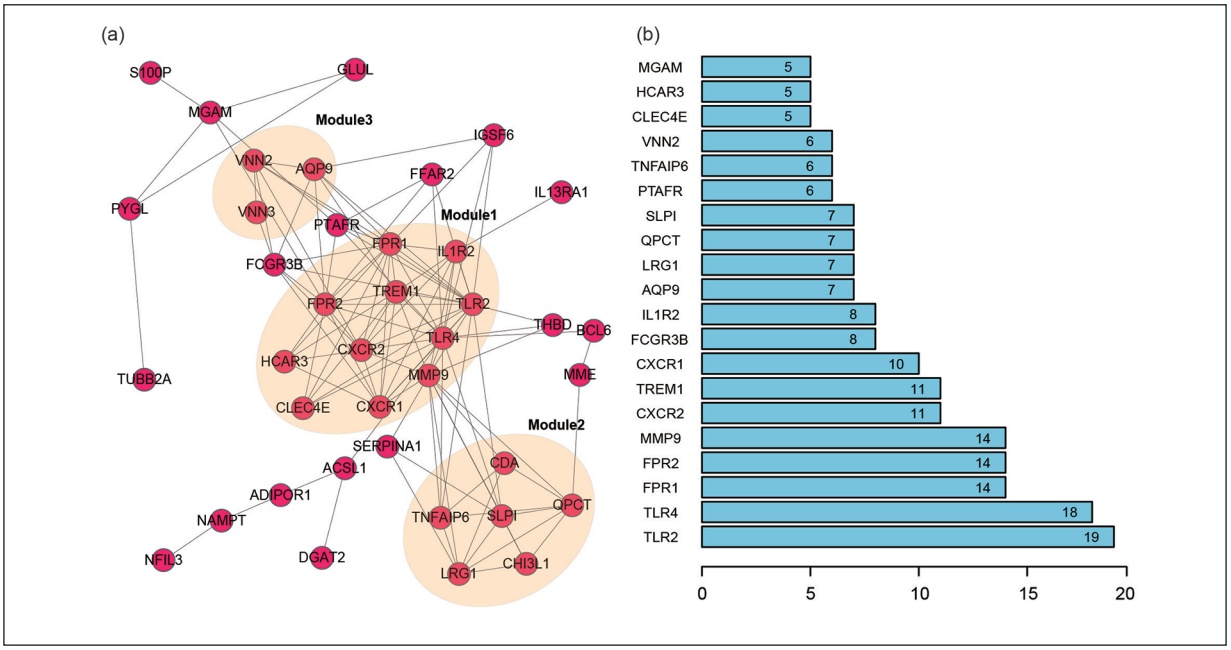

Figure 5. PPI network, modular analyses and histograms of common differentially expressed genes. **A,** The red nodes represent upregulated genes. The most significant module identified by MCODE (score = 8.6). The second most significant module identified by MCODE (score = 4.4). The third most significant module identified by MCODE (score = 3). **B,** Abscissa shows the gene name; ordinate indicates the number of contiguous genes, and height represents the number of gene connections. Abbreviations: MCODE: molecular complex detection; Others: See Figure 1.

and 97 edges (87 miRNAs, 16 upregulated target DEGs, and seven TFs) (Figure 6). In the regulatory network, TLR4 was targeted by SMAD4, and NANOG and LRG1 were targeted by TAF1.

Analyses of the Drug-Gene Network

For hub genes, 163 drug-gene pairs were acquired. In the drug-gene network, there were 153 drugs and 16 genes whose expression was upregulated, including MMP9, CXCR1, MPO, and TLR4 (Figure 7). Drug prediction indicated that the target drug captopril could inhibit MMP9 expression.

Discussion

We revealed the mechanism of the progression of SCAD to AMI. Three datasets were combined into an integrated dataset and classified into two groups: SCAD-Control group and AMI-Control group. Sixty CDEGs were screened out based on the integrated dataset. Another independent GSE59867 dataset was used to confirm the authenticity and reliability of the integrated dataset. Twenty hub genes and three modules were observed in the PPI network. We undertook pathway-enrichment analyses twice using GO and KEGG databases based on the 60 CDEGs and module DEGs, respectively, and the intersection of the results was filtered. Then, we constructed a miRNA-TF-mRNA regulatory network and drug-gene network, which illustrated (at least in part) how SCAD progressed to AMI.

Twenty DEGs were identified as hub genes from the PPI network, of which the five most significant genes were TLR2, TLR4, FPR1, FPR2 and MMP9. These genes were also shown in the three modules, and expression of all of them was upregulated. TLR2 and TLR4 have been demonstrated to be associated with the inflammatory response[29]. Expression of TLR2 and TLR4 has been shown to be higher in MI rats than in sham-operated rats[30]. Besides, TLR polymorphisms have a relationship with CAD risk[31]. FPR2 has been reported to play a crucial part in inflammation resolution, angiogenic responses and cardiac healing[32,33]. FPR1 mRNA shows high expression in rabbits with AMI[34]. MMP9 expression has been shown to be upregulated significantly in CAD samples compared with that in control samples[11].

Based on the miRNA-TF-mRNA regulatory network, we selected miRNAs connecting to ≥2

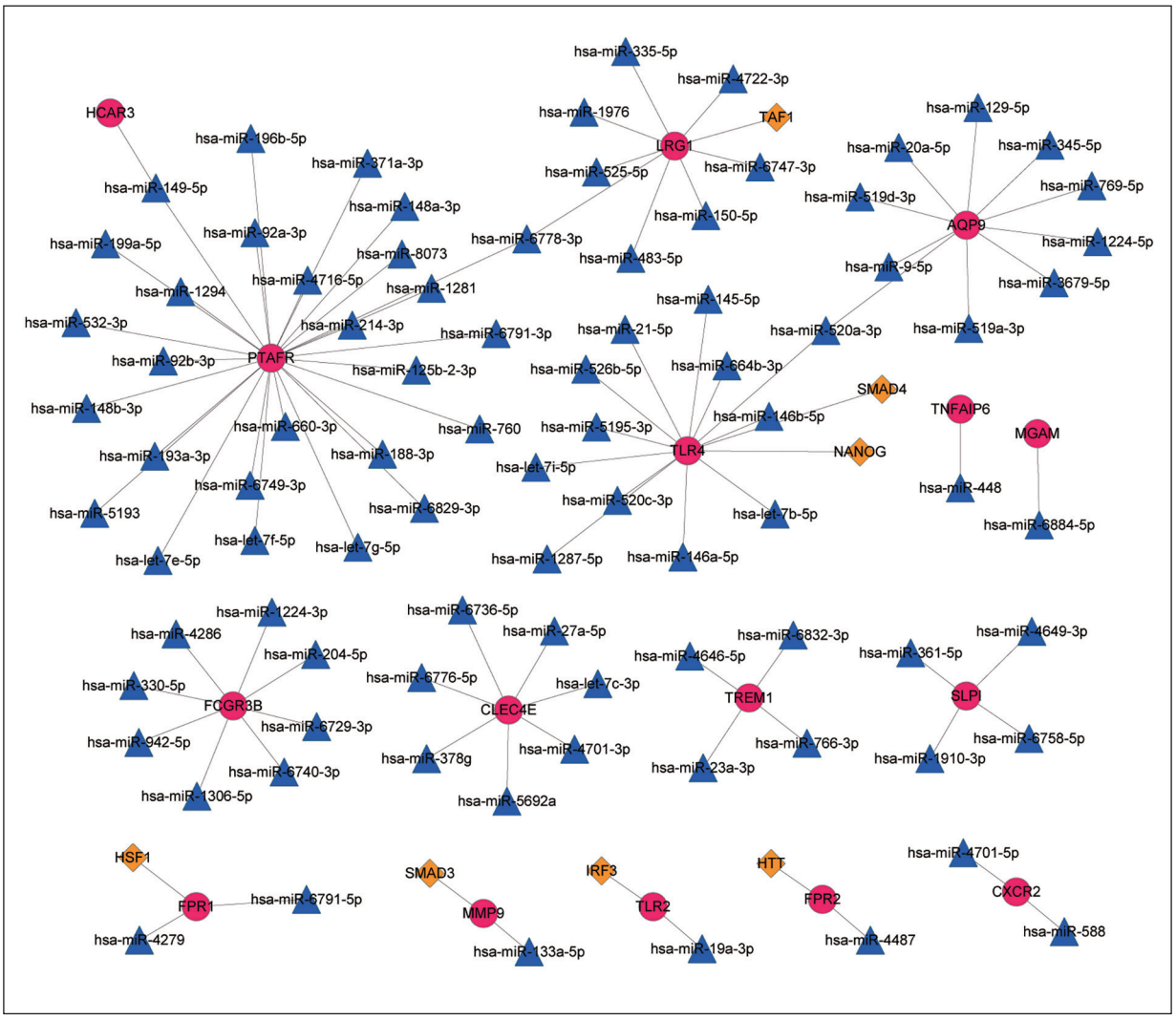

Figure 6. MiRNA-TF-mRNA regulatory network. Red circles, blue triangles, and brown diamonds represent upregulated genes, miRNAs, and TFs, respectively. Abbreviations: See Figure 1.

hub genes and six pairs were identified. Fibrosis and apoptosis were the main causes of the progression from SCAD to AMI[35]. Platelet activating factor receptor (PTAFR) expression has been found to be increased in angiotensin II-induced cardiac fibroblasts; miRNA 30b-5p and miRNA-22-3p can restrain cardiac fibrogenesis after MI by targeting PTAFR[36]. LncRNA PFL competes with miRNA-let-7d to alleviate cardiac fibrosis by targeting PTAFR[37]. Ma et al[38] found that miRNA-149-5p is an apoptosis-related miRNA and is highly expressed in fat-1 transgenic mice after MI surgery. Peng et al[39] discovered that suppression of circDHCR24 expression targets the miRNA-149-5p/MMP9 axis to alleviate aortic the proliferation and migration of smooth muscle cells. Human constitutive androstane receptor (HCAR)3 is a metabolite sensor[40]. Li et al[41] defined HCAR3 to be one of the top genes in the module of CAD by bioinformatics analysis. However, until now, experimental studies have not demonstrated HCAR3 function. We speculate that miRNA-149-5p might target PTAFR and HCAR3 in the progression of SCAD to AMI. Leucine-rich-α2 glycoprotein (LRG)1 has been found to regulate cardiac-fibroblast activation and cardiac fibrosis by interacting with transforming growth factor (TGF)β1, peroxisome proliferator-activated receptor (PPAR)β/δ, and SMRT[42-44]. Studies on miRNA-6778-3p are lacking. We conjecture that miRNA-6778-3p could target LRG1 and PTAFR. AQP9 has been shown to be a

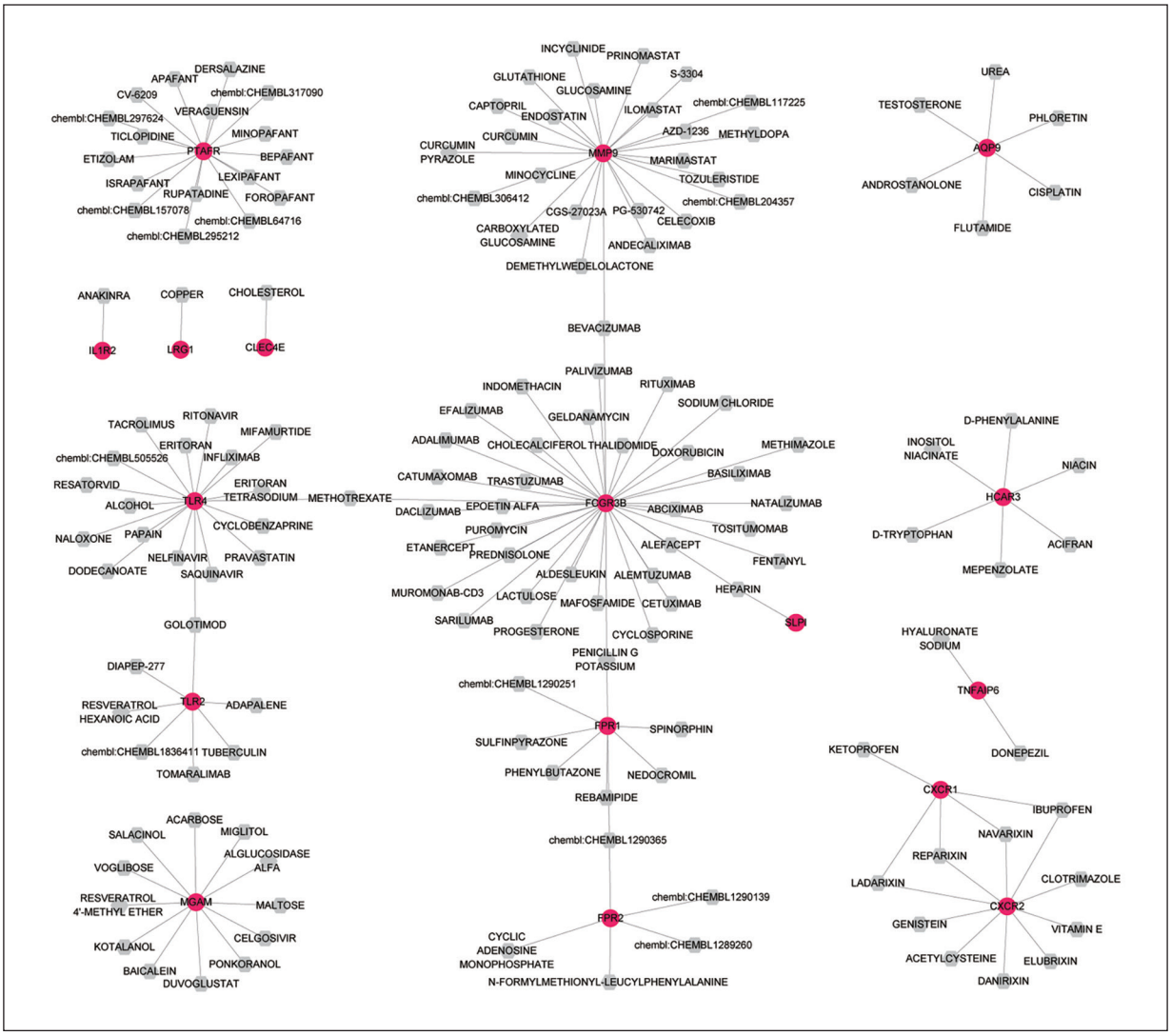

Figure 7. Drug-gene network. Red nodes and gray rectangles represent upregulated genes and drugs, respectively.

potential diagnostic marker of AMI according to RT-qPCR[45]. Studies[46] related to miRNA-520a-3p have been linked to the growth, migration, and invasion of cancer cells. Turner et al[47] discovered the knockdown of SMAD4 expression abolished the stimulatory effects of TGFβ1 on COL4A1/COL4A2 in CAD progression. Scholars[48] have also shown that downregulation of miRNA-224 expression can aggravate cardiac remodeling by targeting the TGFβ/Smad signaling pathway in rats. Therefore, SMAD4 might be involved in the progression of SCAD to AMI by targeting TLR4; miRNA-520a-3p seems to target AQP9 and TLR4 to have a role.

Our study had two main limitations. First, focusing on target genes may lead to exclusion of potential targets. Second, the hypothesis of a miRNA-TF-target regulatory network must be validated experimentally.

Our study revealed the DEGs regulating the progression of CAD and provided new sights for understanding better the genetic inflammatory and immunological CAD pathogenesis. The novelties of our study were as follows. Firstly, after merging the microarray datasets (GSE71226, GSE66360 and GSE97320), we used the "combat" function of "sva" package of R software to remove batch differences. Secondly, we selected the dataset GSE59867 to validate our findings. Thirdly, to make our findings more convinced, four databases were used to predict miRNAs of target genes. Finally, we performed

enrichment analyses and built up PPI network, miRNA-TF-mRNA network and drug-gene network.

Conclusions

We identified several important genes and miRNAs in the progression of SCAD to AMI. We speculate that, in the progression of SCAD to MI: miRNA-149-5p and miRNA-6778-3p might target PTAFR; miRNA-520a-3p might target AQP9 and TLR4/SMAD4; miRNA-149-5p could target HCAR3; miRNA-6778-3p could target LRG1. Besides, inflammation and the immune response played a vital part in the progression of SCAD to AMI.

Conflict of Interest

The Authors declare that they have no conflict of interests.

Funding

This work was supported by the grants from Applied Basic Research Project of Xuzhou to Defeng Pan (grant number: XM12B024).

References

1) David Spence J. Dietary cholesterol and egg yolk should be avoided by patients at risk of vascular disease. J Transl Int Med 2016; 4: 20-24.
2) Kishi S, Magalhaes TA, Cerci RJ, Matheson MB, Vavere A, Tanami Y, Kitslaar PH, George RT, Brinker J, Miller JM, Clouse ME, Lemos PA, Niinuma H, Reiber JH, Rochitte CE, Rybicki FJ, Di Carli MF, Cox C, Lima JA, Arbab-Zadeh A. Total coronary atherosclerotic plaque burden assessment by CT angiography for detecting obstructive coronary artery disease associated with myocardial perfusion abnormalities. J Cardiovasc Comput Tomogr 2016; 10: 121-127.
3) Libby P, Theroux P. Pathophysiology of coronary artery disease. Circulation 2005; 111: 3481-3488.
4) Li GM, Zhang CL, Rui RP, Sun B, Guo W. Bioinformatics analysis of common differential genes of coronary artery disease and ischemic cardiomyopathy. Eur Rev Med Pharmacol Sci 2018; 22: 3553-3569.
5) Rakic M, Persic V, Kehler T, Bastiancic AL, Rosovic I, Laskarin G, Sotosek Tokmadzic V. Possible role of circulating endothelial cells in patients after acute myocardial infarction. Med Hypotheses 2018; 117: 42-46.
6) Rognoni A, Cavallino C, Veia A, Bacchini S, Rosso R, Facchini M, Secco GG, Lupi A, Nardi F, Rametta F, Bongo AS. Pathophysiology of atherosclerotic plaque development. Cardiovasc Hematol Agents Med Chem 2015; 13: 10-13.
7) Szentes V, Gazdag M, Szokodi I, Dézsi CA. The role of CXCR3 and associated chemokines in the development of atherosclerosis and during myocardial infarction. Front Immunol 2018; 9: 1932-1932.
8) Hu G, Ma L, Dong F, Hu X, Liu S, Sun H. Inhibition of microRNA-124-3p protects against acute myocardial infarction by suppressing the apoptosis of cardiomyocytes. Mol Med Rep 2019; 20: 3379-3387.
9) Noori F, Naeimi S, Zibaeenezhad MJ, Gharemirshamlu FR. CCL22 and CCR4 gene polymorphisms in myocardial infarction: risk assessment of rs4359426 and rs2228428 in Iranian population. Clin Lab 2018; 64: 907-913.
10) Kulasingam V, Diamandis EP. Strategies for discovering novel cancer biomarkers through utilization of emerging technologies. Nat Clin Pract Oncol 2008; 5: 588-599.
11) Wang C, Li Q, Yang H, Gao C, Du Q, Zhang C, Zhu L, Li Q. MMP9, CXCR1, TLR6, and MPO participant in the progression of coronary artery disease. J Cell Physiol 2020; 235: 8283-8292.
12) Su J, Gao C, Wang R, Xiao C, Yang M. Genes associated with inflammation and the cell cycle may serve as biomarkers for the diagnosis and prognosis of acute myocardial infarction in a Chinese population. Mol Med Rep 2018; 18: 1311-1322.
13) Vijay K. Toll-like receptors in immunity and inflammatory diseases: past, present, and future. Int Immunopharmacol 2018; 59: 391-412.
14) Barrett T, Wilhite SE, Ledoux P, Evangelista C, Kim IF, Tomashevsky M, Marshall KA, Phillippy KH, Sherman PM, Holko M, Yefanov A, Lee H, Zhang N, Robertson CL, Serova N, Davis S, Soboleva A. NCBI GEO: archive for functional genomics data sets--update. Nucleic Acids Res 2013; 41: D991-995.
15) Gautier L, Cope L, Bolstad BM, Irizarry RA. Affy--analysis of Affymetrix GeneChip data at the probe level. Bioinformatics 2004; 20: 307-315.
16) Leek JT, Johnson WE, Parker HS, Jaffe AE, Storey JD. The sva package for removing batch effects and other unwanted variation in high-throughput experiments. Bioinformatics 2012; 28: 882-883.
17) Choi J. Guide: a desktop application for analysing gene expression data. BMC Genomics 2013; 14: 688.
18) Huang DW, Sherman BT, Tan Q, Collins JR, Alvord WG, Roayaei J, Stephens R, Baseler MW, Lane HC, Lempicki RA. The DAVID Gene Functional Classification Tool: a novel biological module-centric algorithm to functionally analyze large gene lists. Genome Biol 2007; 8: R183.
19) Xie C, Mao X, Huang J, Ding Y, Wu J, Dong S, Kong L, Gao G, Li CY, Wei L. KOBAS 2.0: a web

server for annotation and identification of enriched pathways and diseases. Nucleic Acids Res 2011; 39: W316-322.

20) Kanehisa M, Goto S. KEGG: kyoto encyclopedia of genes and genomes. Nucleic Acids Res 2000; 28: 27-30.

21) Szklarczyk D, Franceschini A, Wyder S, Forslund K, Heller D, Huerta-Cepas J, Simonovic M, Roth A, Santos A, Tsafou KP, Kuhn M, Bork P, Jensen LJ, von Mering C. STRING v10: protein-protein interaction networks, integrated over the tree of life. Nucleic Acids Res 2015; 43: D447-452.

22) Kohl M, Wiese S, Warscheid B. Cytoscape: software for visualization and analysis of biological networks. Methods in molecular biology (Clifton, N.J.) 2011; 696: 291-303.

23) Huang HY, Lin YC, Li J, Huang KY, Shrestha S, Hong HC, Tang Y, Chen YG, Jin CN, Yu Y, Xu JT, Li YM, Cai XX, Zhou ZY, Chen XH, Pei YY, Hu L, Su JJ, Cui SD, Wang F, Xie YY, Ding SY, Luo MF, Chou CH, Chang NW, Chen KW, Cheng YH, Wan XH, Hsu WL, Lee TY, Wei FX, Huang HD. MiRTarBase 2020: updates to the experimentally validated microRNA-target interaction database. Nucleic Acids Res 2020; 48: D148-d154.

24) Sticht C, De La Torre C, Parveen A, Gretz N. miRWalk: An online resource for prediction of microRNA binding sites. PLoS One 2018; 13: e0206239.

25) Li JH, Liu S, Zhou H, Qu LH, Yang JH. starBase v2.0: decoding miRNA-ceRNA, miRNA-ncRNA and protein-RNA interaction networks from large-scale CLIP-Seq data. Nucleic Acids Res 2014; 42: D92-97.

26) Chen Y, Wang X. MiRDB: an online database for prediction of functional microRNA targets. Nucleic Acids Res 2020; 48: D127-d131.

27) Chen EY, Tan CM, Kou Y, Duan Q, Wang Z, Meirelles GV, Clark NR, Ma'ayan A. Enrichr: interactive and collaborative HTML5 gene list enrichment analysis tool. BMC Bioinformatics 2013; 14: 128.

28) Cotto KC, Wagner AH, Feng YY, Kiwala S, Coffman AC, Spies G, Wollam A, Spies NC, Griffith OL, Griffith M. DGIdb 3.0: a redesign and expansion of the drug-gene interaction database. Nucleic Acids Res 2018; 46: D1068-D1073.

29) Rotter Sopasakis V, Sandstedt J, Johansson M, Lundqvist A, Bergström G, Jeppsson A, Mattsson Hultén L. Toll-like receptor-mediated inflammation markers are strongly induced in heart tissue in patients with cardiac disease under both ischemic and non-ischemic conditions. Int J Cardiol 2019; 293: 238-247.

30) Ohno K, Kuno A, Murase H, Muratsubaki S, Miki T, Tanno M, Yano T, Ishikawa S, Yamashita T, Miura T. Diabetes increases the susceptibility to acute kidney injury after myocardial infarction through augmented activation of renal Toll-like receptors in rats. Am J Physiol Heart Circ Physiol 2017; 313: H1130-H1142.

31) Golovkin AS, Ponasenko AV, Khutornaya MV, Kutikhin AG, Salakhov RR, Yuzhalin AE, Zhidkova, II, Barbarash OL, Barbarash LS. Association of TLR and TREM-1 gene polymorphisms with risk of coronary artery disease in a Russian population. Gene 2014; 550: 101-109.

32) Cattaneo F, Parisi M, Ammendola R. Distinct signaling cascades elicited by different formyl peptide receptor 2 (FPR2) agonists. Int J Mol Sci 2013; 14: 7193-7230.

33) Kain V, Jadapalli JK, Tourki B, Halade GV. Inhibition of FPR2 impaired leukocytes recruitment and elicited non-resolving inflammation in acute heart failure. Pharmacol Res 2019; 146: 104295.

34) Zheng M, Liu Z, Liu N, Hou C, Pu J, Zhang S. The effect of Wenxin Keli on the mRNA expression profile of rabbits with myocardial infarction. Evid Based Complement Alternat Med 2016; 2016: 2352614.

35) Shao C, Wang J, Tian J, Tang YD. Coronary artery disease: from mechanism to clinical practice. Adv Exp Med Biol 2020; 1177: 1-36.

36) Zhao XS, Ren Y, Wu Y, Ren HK, Chen H. MiR-30b-5p and miR-22-3p restrain the fibrogenesis of post-myocardial infarction in mice via targeting PTAFR. Eur Rev Med Pharmacol Sci 2020; 24: 3993-4004.

37) Liang H, Pan Z, Zhao X, Liu L, Sun J, Su X, Xu C, Zhou Y, Zhao D, Xu B, Li X, Yang B, Lu Y, Shan H. LncRNA PFL contributes to cardiac fibrosis by acting as a competing endogenous RNA of let-7d. Theranostics 2018; 8: 1180-1194.

38) Ma H, Chen P, Sang C, Huang D, Geng Q, Wang L. Modulation of apoptosis-related microRNAs following myocardial infarction in fat-1 transgenic mice vs wild-type mice. J Cell Mol Med 2018; 22: 5698-5707.

39) Peng W, Li T, Pi S, Huang L, Liu Y. Suppression of circular RNA circDHCR24 alleviates aortic smooth muscle cell proliferation and migration by targeting miR-149-5p/MMP9 axis. Biochem Biophys Res Commun 2020; 529: 753-759.

40) Kapolka NJ, Isom DG. HCAR3: an underexplored metabolite sensor. Nat Rev Drug Discov 2020; 19: 745.

41) Li Y, Lin M, Wang K, Zhan Y, Gu W, Gao G, Huang Y, Chen Y, Huang T, Wang J. A module of multifactor-mediated dysfunction guides the molecular typing of coronary heart disease. Mol Genet Genomic Med 2020: e1415.

42) Liu C, Lim ST, Teo MHY, Tan MSY, Kulkarni MD, Qiu B, Li A, Lal S, Dos Remedios CG, Tan NS, Wahli W, Ferenczi MA, Song W, Hong W, Wang X. Collaborative regulation of LRG1 by TGF-β1 and PPAR-β/δ modulates chronic pressure overload-induced cardiac fibrosis. Circ Heart Fail 2019; 12: e005962.

43) Song W, Wang X. The role of TGFβ1 and LRG1 in cardiac remodelling and heart failure. Biophys Rev 2015; 7: 91-104.

44) Wang X, Abraham S, McKenzie JAG, Jeffs N, Swire M, Tripathi VB, Luhmann UFO, Lange CAK, Zhai Z, Arthur HM, Bainbridge J, Moss SE, Greenwood J. LRG1 promotes angiogenesis by modulating endothelial TGF-β signalling. Nature 2013; 499: 306-311.

45) Chen J, Yu L, Zhang S, Chen X. Network analysis-based approach for exploring the potential diagnostic biomarkers of acute myocardial infarction. Front Physiol 2016; 7: 615.

46) Zhang N, Xing X, Gu F, Zhou G, Liu X, Li B. Ropivacaine inhibits the growth, migration and invasion of gastric cancer through attenuation of WEE1 and PI3K/AKT signaling via miR-520a-3p. Onco Targets Ther 2020; 13: 5309-5321.

47) Turner AW, Nikpay M, Silva A, Lau P, Martinuk A, Linseman TA, Soubeyrand S, McPherson R. Functional interaction between COL4A1/COL4A2 and SMAD3 risk loci for coronary artery disease. Atherosclerosis 2015; 242: 543-552.

48) Xu HM, Sui FH, Sun MH, Guo GL. Downregulated microRNA-224 aggravates vulnerable atherosclerotic plaques and vascular remodeling in acute coronary syndrome through activation of the TGF-β/Smad pathway. J Cell Physiol 2019; 234: 2537-2551.